Optimization of Orbital Trajectory for Frequency Modulated Gyroscope

Sergei A. Zotov, Igor P. Prikhodko, Brent Simon, Alexander A. Trusov, Andrei M. Shkel MicroSystems Laboratory, University of California, Irvine, CA, USA

Abstract—We present the detailed analysis of the orbital trajectory of Frequency Modulated (FM) gyroscopes, and the impact of this on the differential frequency output. The FM approach is based on tracking the resonant frequency split between two, high Q-factor mechanical modes of a Rate Integrating Gyroscope, for the purpose of producing a frequency-based measurement of the input angular rate. We show that the output of FM gyroscopes have a strong dependency on the orbital trajectory. For some orbital trajectories, FM gyroscopes provide inherent self-calibration against common-mode influences, such as temperature and stress, while for other trajectories the gyroscope loses these advantages.

I. Introduction

Commercial MEMS Coriolis Vibratory Gyroscopes (CVG) rely on Amplitude Modulation (AM) of the input stimulus, where the inertial input produces a proportional change in the sensor's output voltage [1]. In this approach, the output analog voltage of a sensor is proportional to the true input stimulus, as well as device parameters, which include stiffness of the springs, gain of pick-off electronics, and other parameters. Variation of these parameters due to changing environmental conditions produces unpredictable drifts in the sensor output.

In contrast to conventional AM MEMS inertial sensors, there is an alternative approach - FM operation. This approach tracks the resonant frequency split between two X-Y modes of vibration in a CVG type II [1], and provides a frequency-based measurement of the input angular rate. As we demonstrated previously in [2], MEMS gyroscopes with mechanical FM operation could eliminate the gain-bandwidth product and dynamic range limitations of conventional AM gyroscopes as well as enable signal-to-noise ratio improvements without limiting the measurement bandwidth. In addition, FM sensor architectures are robust against mechanical and electromagnetic interferences. But the most important advantage of gyroscopes with mechanical FM operation is inherent immunity to variations in temperature, enabled by the real-time selfcalibrating differential frequency detection. Here we utilize the phenomenon that each mode of the gyroscope (X-mode and Y-mode) is a superposition of two harmonics with frequencies $\lambda_1 = \omega_0 + \Omega$ and $\lambda_2 = \omega_0 - \Omega$, while the output FM signal of the gyroscope is $\lambda_1 - \lambda_2 = 2\Omega$. Thus, the FM output of the gyroscope is independent of the natural frequency, ω_0 , which is susceptible to a number of factors which include temperature, stress, and aging of the device.

It is important to note, however, that the degree of selfcalibration varies with the nominal orbital trajectory of the device. Should this trajectory be chosen incorrectly or poorly controlled, little to no self-calibration features will be preserved.

In this paper, we derive and analyze the impact of the orbital trajectory on the differential output of FM gyroscopes. In addition, recommendations are provided for choosing the optimal orbital trajectory to achieve the highest degree of self-compensation.

II. THEORETICAL MODEL FOR CLASS II CVG

Assuming negligible damping, free vibration of a modematched device is governed by

$$-\kappa \dot{\Omega} y + \ddot{x} + (\omega_0^2 - \kappa \Omega^2) x - 2\kappa \Omega \dot{y} = 0,$$

$$\kappa \dot{\Omega} x + \ddot{y} + (\omega_0^2 - \kappa \Omega^2) y + 2\kappa \Omega \dot{x} = 0,$$
 (1)

where ω_0 is the mechanical natural frequency for $\Omega=0$ input, κ is the angular gain defined by the geometric structure of the gyroscope, and in further studies we set $\kappa=1$. The equations (1) are written with respect to a non-inertial frame of reference, attached to the gyroscope die. In the inertial frame, the governing equations can be represented as follows:

$$\ddot{\xi} + \omega_0^2 x = 0, \quad \ddot{\eta} + \omega_0^2 y = 0.$$
 (2)

Depending on the initial conditions, the solution of (2) corresponds to an orbital trajectory in the form of either a line, an ellipse, or a circle. This pattern remains stationary in the inertial space (for the case when $\kappa < 1$ the pattern rotates in the inertial space with a rate $(1-\kappa)\Omega(t)$). This phenomenon can be used for realization of a whole angle gyroscope [3] or a FM rate gyroscope [2]. The solution of (2) for a normalized amplitude is

$$\xi = \sin(\omega_0 t), \quad \eta = \sin(\omega_0 t + \phi),$$
 (3)

where the initial phase, ϕ , defines the orbital trajectory in the inertial space: for $\phi=0,\pm180^{\circ}$ – line, for $\phi=\pm90^{\circ}$ – circle, and an ellipse for any other value of ϕ .

Mapping solution (3) back to the non-inertial reference frame attached to the gyroscope die

$$x = \sin(\omega_0 t)\cos(\Omega t) + \sin(\omega_0 t + \phi)\sin(\Omega t),$$

$$y = -\sin(\omega_0 t)\sin(\Omega t) + \sin(\omega_0 t + \phi)\cos(\Omega t),$$
(4)

following the trigonometric transformation of the solution (4), it can be re-written as:

$$x = A_{\omega+\Omega} \sin\left((\omega_0 + \Omega)t + \Phi_1\right)$$

$$+A_{\omega-\Omega} \sin\left((\omega_0 - \Omega)t + \Phi_2\right),$$

$$y = A_{\omega+\Omega} \sin\left((\omega_0 + \Omega)t + \Phi_3\right)$$

$$+A_{\omega-\Omega} \sin\left((\omega_0 - \Omega)t + \Phi_4\right),$$
(5)

where

$$A_{\omega+\Omega} = \frac{\sqrt{2}}{2}\sqrt{1+\sin(\phi)}, A_{\omega-\Omega} = \frac{\sqrt{2}}{2}\sqrt{1-\sin(\phi)} \quad (6)$$

$$\Phi_{1} = -\arcsin\left(\frac{\cos(\phi)}{A_{\omega+\Omega}/2}\right), \Phi_{2} = \arcsin\left(\frac{\cos(\phi)}{A_{\omega-\Omega}/2}\right), \\
\Phi_{3} = -\arcsin\left(\frac{1+\sin(\phi)}{A_{\omega+\Omega}/2}\right), \Phi_{4} = \arcsin\left(\frac{1-\sin(\phi)}{A_{\omega-\Omega}/2}\right).$$
(7)

Expressions for x and y in (5) define the gyroscope dynamics with respect to a rotating frame of reference attached to the gyroscope die as a superposition of two sinusoids with frequencies $\omega_0 + \Omega$ and $\omega_0 - \Omega$. Thus, the amplitudes of each sinusoid (6) defines the orbital trajectory through parameter ϕ . When $\dot{\Omega} \neq 0$, the phases in (5) are $\omega_0 t \pm \int_0^t \Omega(t) dt + \Phi_i$, while the instantaneous frequencies, which are defined by the time derivative of the phase, remain as $\omega_0 \pm \Omega$.

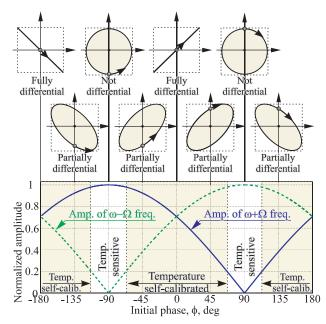
Fig. 1 shows the value of the amplitudes $A_{\omega+\Omega}$ and $A_{\omega-\Omega}$ which corresponds to the frequencies $\omega_0 + \Omega$ and $\omega - \Omega$, respectively. Depending on the initial phase, ϕ , we can see three distinct gyro orbital trajectories: line, ellipse or circle:

- 1) $\phi=0$ or $\phi=\pm 180^\circ$. Orbital trajectory is a line. The amplitudes of each sinusoid are equal, $A_{\omega+\Omega}=A_{\omega-\Omega}$. In this mode the gyroscope provides fully differential operation, with the greatest factor of inherent self-calibration.
- 2) $\phi>0$ and $\phi<180^\circ$. Orbital trajectory is an ellipse with clockwise vibration. The amplitudes of each sinusoid are not equal $A_{\omega+\Omega}< A_{\omega-\Omega}$.
- 3) $\phi < 0$ and $\phi > -180^{\circ}$. Orbital trajectory is an ellipse with counter-clockwise vibration. The amplitudes of each sinusoid are not equal $A_{\omega+\Omega} > A_{\omega-\Omega}$.
- 4) $\phi=\pm90^\circ$. Orbital trajectory is a circle with clockwise (counter-clockwise for $\phi=-90^\circ$) vibration. Amplitude of the sinusoid with frequency $\omega\pm\Omega$ is equal to zero, $A_{\omega\pm\Omega}=0$. Not differential mode.

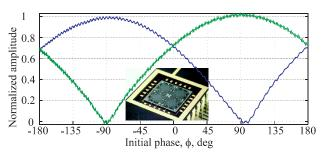
The most beneficial orbital trajectories for the FM gyroscope is when the orbit collapses to a line. In this scenario, we can take full advantage of the differential output signal, providing the greatest degree of inherent self-calibration [2].

In the case when the orbital trajectories is an ellipse, the gyroscope provides a partial differential operation, still preserving the benefits of self-calibration.

When the orbital trajectories is a circle (the last case), the gyroscope is no longer differential and completely looses



(a) Numerical simulation using equations (5)-(6).



(b) Experimental characterization using Quadruple Mass Gyroscope [2].

Fig. 1. Amplitude vs. Orbital Trajectories of FM Gyroscope.

its inherent self-calibration against changes in resonance frequency. In this scenario, the gyroscope remains sensitive to temperature fluctuations and stress, as shown in [4].

III. CONCLUSION

We presented a unified analysis of FM gyroscopes. We demonstrated that orbital trajectory in the form of a line takes full advantage of the differential FM output signal, providing the greatest degree of inherent self-calibration, as shown in [2]. In contrast, when pattern is a circle, the FM gyroscope had only one output frequency, loosing its self-calibration features and becoming highly sensitive to temperature fluctuations [4].

REFERENCES

- Andrei M. Shkel, "Type I and type II micromachined vibratory gyroscopes," in Proc. of IEEE/ION PLANS, 2006, pp. 586-593.
- [2] Sergei A. Zotov, Alexander A. Trusov, Andrei M. Shkel, "High-Range Angular Rate Sensor Based on Mechanical Frequency Modulation," IEEE J. Microelectromech. Syst., vol. 21, no. 2, pp. 398-405, 2012.
- [3] Igor P. Prikhodko, Sergei A. Zotov, Alexander A. Trusov, Andrei M. Shkel, "Foucault pendulum on a chip: Rate integrating silicon MEMS gyroscope," Sensors and Actuators A: Physical, Vol. 177, pp. 67-78, 2012.
- [4] Mitchell H. Kline, Yu-Ching Yeh, Burak Eminoglu, Hadi Najar, Mike Daneman, David A. Horsley, and Bernhard E. Boser "Quadrature FM Gyroscope", Proc. of IEEE MEMS conference, Jan. 2013, pp. 604-608.